

# Controlled Assembly of Magnetic Nanoparticles from Magnetotactic Bacteria Using Microelectromagnets Arrays

Hakho Lee, Alfreda M. Purdon, Vincent Chu, and Robert M. Westervelt\*

Department of Physics and Division of Engineering and Applied Sciences, Harvard University, Cambridge, Massachusetts 02138

Received March 19, 2004; Revised Manuscript Received March 31, 2004

## ABSTRACT

Controlled assembly of magnetic nanoparticles was demonstrated by manipulating magnetotactic bacteria in a fluid with microelectromagnets. Magnetotactic bacteria synthesize a chain of magnetic nanoparticles inside their bodies. Microelectromagnets, consisting of multiple layers of lithographically patterned conductors, generate versatile magnetic fields on micrometer length scales, allowing sophisticated control of magnetotactic bacteria inside a microfluidic chamber. A single bacterium was stably trapped and its orientation was controlled; multiple groups of bacteria were assembled in a fluid. After positioning the bacteria, their cellular membranes were removed by cell lysis, leaving a chain and a ring of magnetic nanoparticles on a substrate.

With the advent of the controlled synthesis of nanocrystals, efforts are being made to assemble these particles into custom-made structures.<sup>1–3</sup> By trapping metallic or semiconducting nanoparticles between electrodes, single-electron devices were constructed.<sup>4,5</sup> Genetically engineered viruses were used to assemble semiconducting nanocrystals into ordered structures.<sup>6,7</sup> The manipulation of magnetic nanoparticles is also of significant interest because single-domain magnets have applications in spintronics, magnetic memory, and biology.<sup>8–10</sup> Using either permanent magnets or electromagnets, various magnetic objects, including magnetic nanowires and superparamagnetic particles, were positioned or moved in a fluid.<sup>11,12</sup>

In this letter, we describe a new approach to assemble magnetic nanoparticles into ordered structures by controlling the motion of magnetotactic bacteria with microelectromagnets. Through highly controlled biomineralization, magnetotactic bacteria synthesize chains of intracellular, single-domain magnetic nanoparticles.<sup>13</sup> The cellular bodies enclosing the magnetic chains prevent the magnetic aggregation of the bacteria, making it possible to use the bacteria as a carrier of magnetic nanoparticles. The microelectromagnets create versatile magnetic field patterns on micrometer length scales to guide the motion of magnetotactic bacteria inside a microfluidic chamber.<sup>14</sup> After assembling the bacteria with microelectromagnets, the cellular membranes of the bacteria

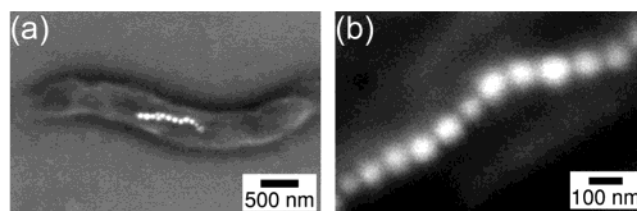


**Figure 1.** Scanning electron micrographs of *Magnetospirillum magnetotacticum* (MS-1). (a) The bacteria synthesize a chain of magnetite ( $\text{Fe}_3\text{O}_4$ ) nanoparticles, which is anchored inside their body. (b) Close-up of the chain of magnetite nanoparticles. Each particle in the chain is covered with a membrane and has magnetic moment  $\sim 6 \times 10^{-17} \text{ A}\cdot\text{m}^2$ . The total magnetic moment of a bacterium is  $\sim 1.0 \times 10^{-15} \text{ A}\cdot\text{m}^2$ .

were removed by cell lysis to leave the biogenic magnetic nanoparticles at desired locations.

The novel magnetic structures produced by magnetotactic bacteria have been a subject of active study since their discovery.<sup>13,15–17</sup> Magnetotactic bacteria grow magnetic nanoparticles inside their bodies. The mineralization processes are highly regulated by the bacteria, leading to the formation of uniform, species-specific magnetic nanoparticles. Moreover, the particles are assembled into single or multiple chains and anchored inside the cell, enabling the bacteria to passively orient themselves along geomagnetic field lines. Figure 1 shows *Magnetospirillum magnetotacticum* (MS-1), a variety of magnetotactic bacteria that grow a single chain of intracellular magnetite ( $\text{Fe}_3\text{O}_4$ ) nanoparticles. Each nanoparticle, which is contained in a phospholipid

\* Corresponding author. E-mail: westervelt@deas.harvard.edu

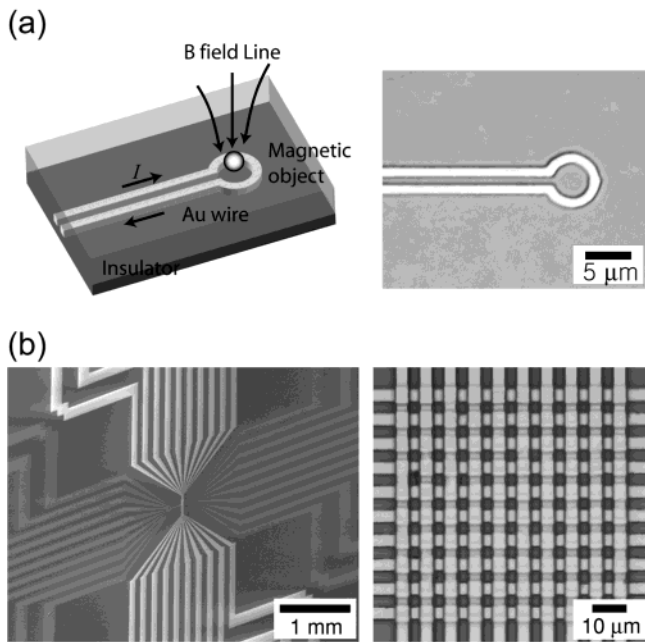


**Figure 2.** Schematic and micrographs of microelectromagnets before attaching microfluidic chambers. (a) A ring trap is a circular Au wire topped with an insulating layer. The current  $I$  in the wire generates a local magnetic peak that traps magnetic objects on the surface of the device (left). A ring trap of diameter  $5 \mu\text{m}$  was fabricated on a Si/SiO<sub>2</sub> substrate (right). (b) A microelectromagnet matrix with electrical leads (left) and its close-up (right). Two layers of 10 Au wires are aligned perpendicular to each other, separated and topped by insulating layers. The width and the pitch of the wires are  $5 \mu\text{m}$  and  $10 \mu\text{m}$ , respectively.

membrane, has a cuboctahedral  $\{111\} + \{100\}$  crystal structure with a narrow size distribution.<sup>15</sup> Furthermore, the diameter of the particle ( $\approx 50 \text{ nm}$ ) falls in a range where the particle is a single-domain permanent magnet with magnetic moment  $\sim 6 \times 10^{-17} \text{ A}\cdot\text{m}^2$ . Adding up the individual magnetic moments of particles in the chain, the total magnetic moment of a single MS-1 bacterium is  $\sim 1.0 \times 10^{-15} \text{ A}\cdot\text{m}^2$ . The cellular bodies enclosing the magnetic chain prevent the clustering of bacteria from magnetic dipole interactions.

To manipulate and assemble magnetotactic bacteria in a fluid, a micromanipulation system was developed using microelectromagnets and microfluidics. The microelectromagnets generate strong, localized magnetic field peaks to precisely position magnetotactic bacteria in a fluid at room temperature. The microfluidic system controls the fluidic flow, which is crucial for the stable trapping of the bacteria. Figure 2 shows two types of microelectromagnets used in the experiment, a ring trap and a matrix, before microfluidic chambers were attached. The ring trap is a circular conducting wire covered with an insulating layer. The matrix consists of two arrays of straight conducting wires, aligned perpendicular to each other, which are separated and capped with insulating layers. The microelectromagnets were fabricated on Si/SiO<sub>2</sub> substrate as previously reported.<sup>14</sup> Conducting wires were patterned using either optical lithography or electron beam lithography followed by Cr/Au deposition and lift-off. To reduce the friction between the trapped bacteria

and the surface of the device, a resin with good planarization properties was used for the insulating layers. A microfluidic chamber was separately fabricated from poly(dimethylsiloxane)s (PDMS) using soft lithography.<sup>18</sup> The width ( $1 \text{ mm}$ ) and the depth ( $100 \mu\text{m}$ ) of the channel were chosen such that the viscous drag on the bacteria by the fluid flow is  $< 10 \text{ pN}$ . The microelectromagnets and the PDMS chamber were treated with an O<sub>2</sub> plasma to render their surfaces hydrophilic, and the chamber was conformally sealed on top of the microelectromagnets.

With currents in the wires, the microelectromagnets generate a local magnetic field peak that traps magnetic objects suspended in a fluid as illustrated in Figure 2a. The magnitude of the magnetic field on the surface of the device is  $B \propto JA/d$ , where  $J$  is the current density,  $A$  is the cross sectional area of the wire, and  $d$  is the distance between the wire and the surface of the device. For the microelectromagnet reported here ( $A = 2 \mu\text{m}^2$  and  $d = 2 \mu\text{m}$ ), current densities as high as  $5 \times 10^7 \text{ A/cm}^2$  were achieved, producing magnetic field magnitudes up to  $B \sim 0.1 \text{ T}$ . The device was cooled by a thermoelectric cooler to prevent thermal breakdown, from Joule heating, and electromigration.

The potential energy of a trapped magnetic object is  $U = -mB$ , where  $m$  is the magnetic moment of the object. In thermal equilibrium, the chemical potentials of magnetic objects inside and outside of a trap are equal to each other. This condition determines the number density of magnetic objects inside a trap  $n_T = n_0 \exp(|U|/k_B T)$ , where  $k_B$  is the Boltzmann constant,  $T$  is the temperature, and  $n_0$  is the number density of magnetic objects outside the trap. In a magnetic trap with trapping volume  $V_T$ , one or more objects will be trapped provided  $n_0 V_T \geq \exp(-|U|/k_B T)$ , which determines the minimum magnetic moment  $m_0 = -(k_B T/B) \cdot \log(n_0 V_T)$  required for stable trapping at a given temperature. Using the experimental conditions reported here,  $n_0 = 10^{-7} / \mu\text{m}^3$ ,  $V_T = 25 \mu\text{m}^3$ , and  $T = 288 \text{ K}$ , the minimum magnetic moment for stable trapping is  $m_0 = 5 \times 10^{-19} \text{ A}\cdot\text{m}^2$  with  $B = 0.1 \text{ T}$ . Because each MS-1 bacterium has the magnetic moment  $\sim 1.0 \times 10^{-15} \text{ A}\cdot\text{m}^2$ , well above the required minimum, it can be stably trapped and manipulated with microelectromagnets.

As a first step to assemble magnetic nanoparticles, MS-1 bacteria were manipulated inside the microfluidic chamber using microelectromagnets as shown in Figure 3. The bacteria were stained with fluorescent dye and the manipulation process was monitored with a fluorescent microscope. A solution containing the stained bacteria was introduced into the microfluidic chamber above the microelectromagnet by a low flow-rate peristaltic pump. A single current source was connected to a ring trap; each wire in a matrix was connected to a separate current source that was individually controlled by a computer.

The sequence of images in Figure 3a shows the trapping of a single MS-1 bacterium by a ring trap with  $B = 6 \text{ mT}$  at the center. Once trapped, the bacterium underwent complex motions due to its own motility, but it remained trapped as long as the magnetic field was on. By controlling the current in each wire of the matrix, more versatile manipulation of

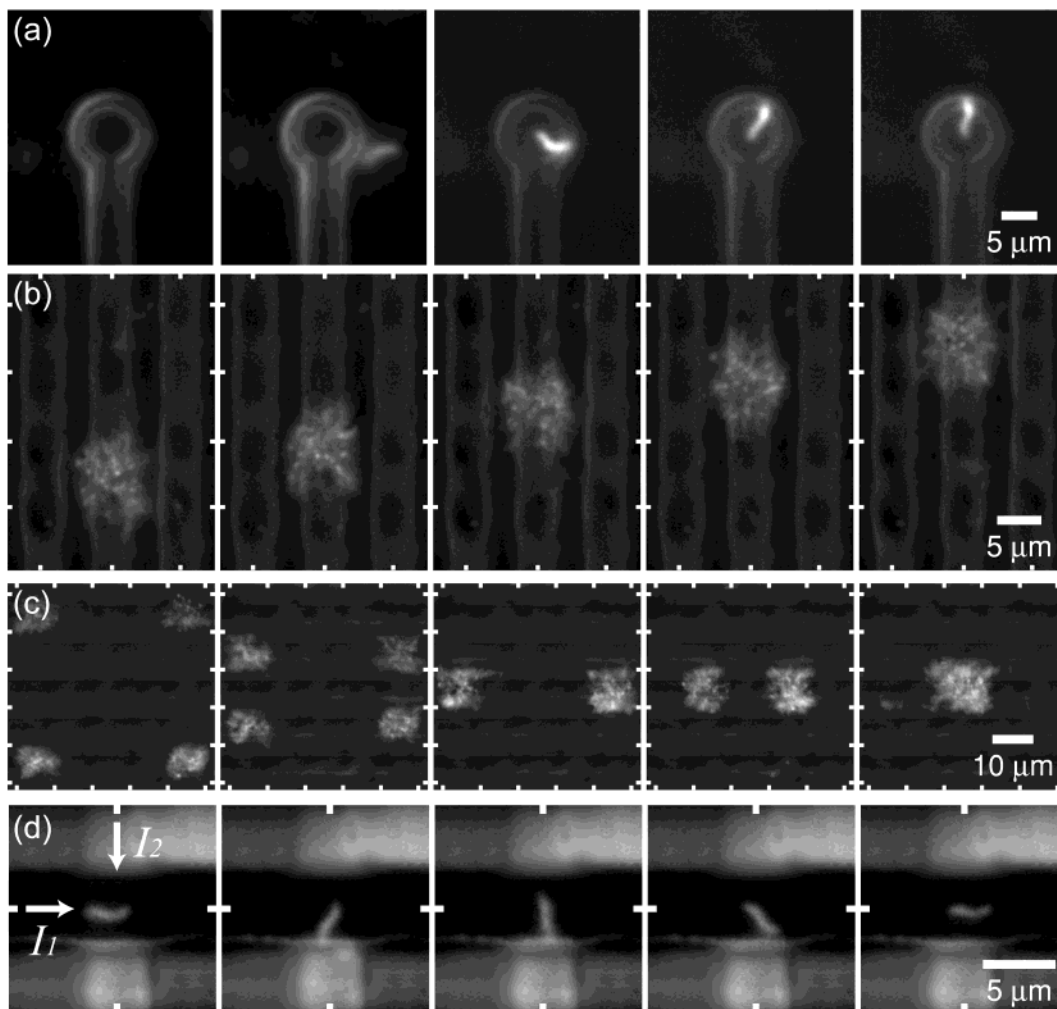


**Figure 3.** Micromanipulation of *Magnetospirillum magnetotacticum* (MS-1) with microelectromagnets. (a) A single MS-1 bacterium was trapped at the center of the ring ( $B = 6$  mT). The bacterium remained inside the trap as long as the magnetic field was on. By adjusting the currents in wires, the microelectromagnet matrix provided more versatile manipulation. (b) A single peak in the magnetic field magnitude was created and moved in steps less than the wire pitch, trapping and transporting a group of MS-1 bacteria continuously across the surface of the device. (c) Assembly of magnetotactic bacteria. Four groups of bacteria were separately trapped and brought together into a single group. (d) The direction of a trapped bacterium was controlled by applying two sinusoidal currents,  $I_1$  and  $I_2$  with a  $\pi/2$  phase difference. White ticks indicate the wire positions.

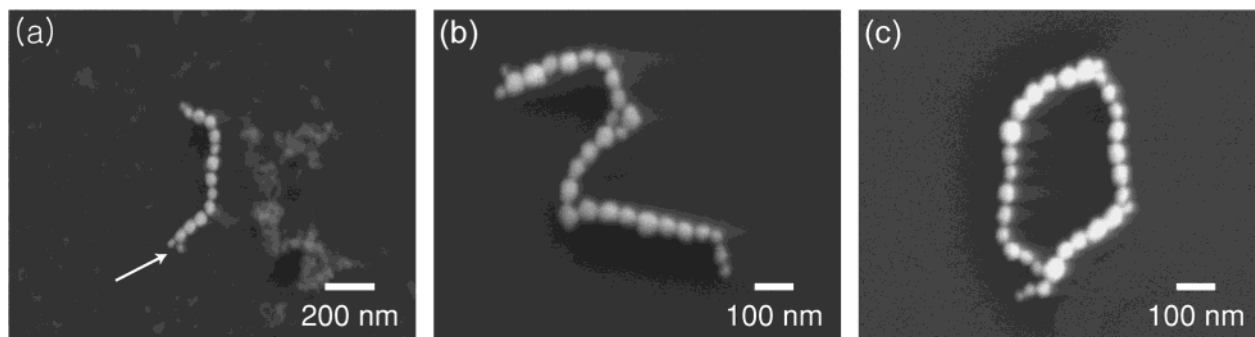


**Figure 4.** Scanning electron micrographs of assembled magnetic structures after removing cellular membrane of trapped bacteria. (a) A single chain of magnetic nanoparticles is shown along with cellular debris. Two small nanoparticles indicated by an arrow are still attached to the chain due to the magnetic field from the adjacent, large particle. (b) A long chain from a single bacterium. The chain bent during the cell lysis but remained intact from the strong magnetic dipole interactions among nanoparticles. (c) A ring of magnetic nanoparticles was formed by trapping and lysing two bacteria. The cellular bodies enclosing the magnetic chains prevented clustering of the chains during trapping and cell lysis.

bacteria was performed. In Figure 3b, a single peak in the magnetic field magnitude was created and moved in steps less than the wire pitch of the matrix, trapping and continu-

ously transporting a group of bacteria. Multiple groups of bacteria were independently moved along different paths as shown in Figure 3c; after initially trapping four groups of

bacteria, each group was moved independently to form a single large group. In addition to trapping a bacterium, the matrix can further control the orientation of the bacterium as shown in Figure 3d. Sinusoidal currents with a  $\pi/2$  phase difference were applied to two wires crossing each other. By changing the phase of the currents, a single bacterium was rotated on the surface of the device at the crossing point of the two wires.

After positioning MS-1 bacteria with microelectromagnets, the cellular membranes of the bacteria were removed by cell lysis to expose the assembled magnetic nanostructures. The microfluidic chamber was drained, leaving the trapped bacteria on the surface of the device. The trapped bacteria were treated with distilled water to burst the cells by osmotic shock. Subsequently, sodium dodecyl sulfate (SDS) solution (20% weight/volume) was introduced to remove the remaining cellular membranes and debris. Finally, distilled water was introduced again to dissolve the residue of SDS.

Figure 4 shows the examples of magnetic structures left on the substrate after removing the cellular membrane of trapped MS-1 bacteria. In Figure 4a, a chain of magnetic nanoparticles from a single bacterium is shown along with cellular debris. Two small nanomagnets at the lower end of the chain are noteworthy. Left alone, the magnetic moment of these particles is expected to fluctuate at room temperature. However, due to the magnetic field from the adjacent large particle, the magnetic moments of the small particles are aligned and the particles are attached to the chain.<sup>19</sup> The length of the magnetic chain can be different in each bacterium. Figure 4b shows a long chain from a single bacterium. The chain, initially straight, bent during the lysis process, but it remained intact due to the strong magnetic interactions between magnetic nanoparticles. Figure 4c shows a more complex structure, a ring of magnetic nanoparticles assembled from two magnetic chains. Because each magnetic chain was initially enclosed in a bacterial body, it maintained its linear geometry during trapping and cell lysis. These ordered magnetic structures can serve as a system for studying the interactions between closely spaced magnetic nanoparticles.

By manipulating magnetotactic bacteria with microelectromagnets, we demonstrated how magnetic nanoparticles grown by the bacteria can be assembled into ordered structures. Using an electric field for manipulation, the method described above can be extended to assemble other types of biogenic nanoparticles, for example, silver or gold nanocrystals in bacteria, or cadmium sulfide nanocrystals in yeast.<sup>20–22</sup> By applying an ac electric field, the microorganisms containing nanoparticles can be trapped and positioned by dielectrophoretic force.<sup>23,24</sup> Subsequent removal of the cellular bodies can expose the intracellular nanoparticles at

desired locations. Combing biomineralization and micromanipulation, this approach can be a new method for growing and assembling nanoparticles into customized structures.

**Acknowledgment.** We thank X. Zhuang and M. Bawendi for their helpful comments. This work was supported by the Nanoscale Science and Engineering Center at Harvard under NSF grant PHY-0117795.

## References

- (1) Puentes, V. F.; Krishnan, K. M.; Alivisatos, A. P. *Science* **2001**, *291*, 2115–2117.
- (2) Malynych, S.; Robuck, H.; Chumanov, G. *Nano Lett.* **2001**, *1*, 647–649.
- (3) Klimov, V. I.; Mikhailovsky, A. A.; Xu, S.; Malko, A.; Hollingsworth, J. A.; Leatherdale, C. A.; Eisler, H.; Bawendi, M. G. *Science* **2000**, *290*, 314–317.
- (4) Wu, C. S.; Chen, C. D.; Shih, S. M.; Su, W. F. *Appl. Phys. Lett.* **2002**, *81*, 4595–4597.
- (5) Mao, C.; Flynn, C. E.; Lim, A. K. L.; Alivisatos, A. P.; McEuen, P. L. *Nature* **1997**, *389*, 699–701.
- (6) Lee, S. W.; Mao, C.; Flynn, C. E.; Belcher, A. M. *Science* **2002**, *296*, 892–895.
- (7) Mao, C.; Flynn, C. E.; Hayhurst, A.; Sweeney, R.; Qi, J.; Georgiou, G.; Iverson, B.; Belcher, A. M. *Proc. Natl. Acad. Sci. U.S.A.* **2003**, *100*, 6946–6951.
- (8) Black, C. T.; Murray, C. B.; Sandstrom, R. L.; Sun, S. *Science* **2000**, *290*, 1131–1134.
- (9) Sun, S.; Murray, C. B.; Weller, D.; Folks, L.; Moser, A. *Science* **2000**, *287*, 1989–1991.
- (10) Häfeli, U. *Scientific and clinical applications of magnetic carriers*; Plenum Press: New York, 1997.
- (11) Tanase, M.; Silevitch, D. M.; Hultgren, A.; Bauer, L. A.; Searson, P. C.; Meyer, G. J.; Reich, D. H. *J. Appl. Phys.* **2002**, *91*, 8549–8551.
- (12) Barbic, M.; Mock, J. J.; Gray, A. P.; Schultz, S. *Appl. Phys. Lett.* **2001**, *79*, 1897–1899.
- (13) Blakemore, R. *Science* **1975**, *190*, 377–379.
- (14) Lee, C. S.; Lee, H.; Westervelt, R. M. *Appl. Phys. Lett.* **2001**, *79*, 3308–3310.
- (15) Frankel, R. B.; Blakemore, R. P.; Wolfe, R. S. *Science* **1979**, *203*, 1355–1356.
- (16) Matsunaga, T. *Trends Biotechnol.* **1991**, *9*, 91–95.
- (17) Ofer, S.; Nowik, I.; Bauminger, E. R.; Papaefthymiou, G. C.; Frankel, R. B.; Blakemore, R. P. *Biophys. J.* **1984**, *46*, 57–64.
- (18) Whitesides, G. M.; Ostuni, E.; Takayama, S.; Jiang, X.; Ingber, D. E. *Annu. Rev. Biomed. Eng.* **2001**, *3*, 335–373.
- (19) Dunin-Borkowski, R. E.; McCartney, M. R.; Frankel, R. B.; Bazylinski, D. A.; Posfai, M.; Buseck, P. R. *Science* **1998**, *282*, 1868–1870.
- (20) Klaus, T.; Joerger, R.; Olsson, E.; Granqvist, C. G. *Proc. Natl. Acad. Sci. U.S.A.* **1999**, *96*, 13611–13614.
- (21) Ahmad, A.; Senapati, S.; Islam Khan, M.; Kumar, R.; Ramani, R.; Srinivas, V.; Sastry, M. *Nanotechnology* **2003**, *14*, 824–828.
- (22) Dameron, C. T.; Reese, R. N.; Mehra, R. K.; Kortan, A. R.; Carroll, P. J.; Steigerwald, M. L.; Brus, L. E.; Winge, D. R. *Nature* **1989**, *338*, 596–597.
- (23) Pohl, H. A. *Dielectrophoresis: the behavior of neutral matter in nonuniform electric fields*; Cambridge University Press: Cambridge, 1978.
- (24) Hughes, M. P. *Nanoelectromechanics in engineering and biology*; CRC Press: Boca Raton, 2003.

NL049562X